

^{38}K isomer production via fast fragmentation

K. A. Chipps,¹ R. L. Kozub,² C. Sumithrarachchi,³ T. Ginter,³ T. Baumann,³ K. Lund,³
 A. Lapierre,³ A. Villari,³ F. Montes,^{4,3} S. Jin,^{4,3,5} K. Schmidt,^{4,3} S. Ayoub,^{4,3}
 S. D. Pain,¹ and D. Blankstein⁶

¹*Oak Ridge National Laboratory, Oak Ridge, Tennessee 37831, USA*

²*Tennessee Technological University, Cookeville, Tennessee 38505, USA*

³*National Superconducting Cyclotron Laboratory, East Lansing, Michigan 48824, USA*

⁴*Michigan State University, East Lansing, Michigan 48824, USA*

⁵*Institute of Modern Physics, Chinese Academy of Science, Lanzhou 730000, China,*

⁶*University of Notre Dame, Notre Dame, Indiana 46556, USA*



(Received 25 September 2018; published 6 December 2018)

In radioactive ion beam experiments, beams containing isomers can be of interest in probing nuclear structure and informing astrophysical reaction rates. While the production of mixed in-flight ground state and isomer beams using nucleon transfer can be generally understood through distorted wave Born approximation methodology, low-spin isomer production via fast fragmentation is relatively unstudied. To attain a practical understanding of low-spin isomer production using fast fragmentation beams, a test case of $^{38}\text{K}/^{38m}\text{K}$ was studied at the National Superconducting Cyclotron Laboratory's ReAccelerated Beam facility. Starting from LISE++ predictions, the fragmentation momentum distribution was sampled to determine isomer production. In addition, the effects of the gas stopper gradient and charge breeding times were examined. In the case of ^{38}K , isomer production peaks at $\sim 57\%$. This maximum is observed just off the LISE++ predicted optimum magnetic rigidity, with only small losses in beam intensity within a few percent of this optimum rigidity setting. Control of the isomer fraction was also achieved through the modification of charge breeding times. Fast fragmentation appears to be a feasible method for production of low-spin isomeric beams, but additional study is necessary to better describe the mechanism involved.

DOI: 10.1103/PhysRevAccelBeams.21.121301

I. INTRODUCTION

As techniques for producing radioactive ion beams continue to improve, additional opportunities arise. Among these is the possibility to study nuclear reactions on strongly populated isomeric states within the beam. In some cases, an isomer may be of interest for probing otherwise inaccessible nuclear structure information [1–4]; in other cases, such as ^{26}Al and ^{38}K , astrophysical reactions on the isomer can play an important role in the reaction network [5].

The techniques necessary for creating mixed ground state and isomer ($g + i$) beams, however, have not been thoroughly explored. The population of low-lying isomeric states using nucleon transfer at a few to tens of MeV/u (see, for example, Refs. [5,6]) can be reasonably well understood using distorted wave Born approximation formalism. Isomeric beams have also been demonstrated using the isotope production online technique (e.g., [1]), with

selection [2] and postacceleration [3] being achieved with the application of resonant laser ionization. In fragmentation reactions on fast beams, however, low-spin isomer production is not well reproduced by models, though higher spins in higher mass regions are more accurately predicted (see, for example, Ref. [7]); fast beam fragmentation is generally used in large-scale searches for high-spin isomers [8–11], though it has been observed to produce medium-spin isomers as well [12]. However, fast fragmentation has several potential benefits over production via in-flight transfer reactions: Instead of having to retune the driver (primary) beam energy to the peak of the differential cross section for each ℓ transfer, a single beam energy can be utilized for relatively similar production of both the ground state and isomer; and the techniques used to stop and reaccelerate the fragmentation beam can be used directly to alter the ground state to isomeric ratio.

In the current work, ^{38}K was studied as an example case for the production of low-spin isomer beams using fast fragmentation. ^{38}K contains a 0^+ isomer at 130.4 keV [13] in addition to its 3^+ ground state. ^{38}K is of particular interest for beam development, as the $^{38}\text{K}(p,\gamma)^{39}\text{Ca}$ reaction is an important link in the astrophysical rp process, and the nucleosynthetic flow is bottlenecked by the beta decay of

Published by the American Physical Society under the terms of the *Creative Commons Attribution 4.0 International license*. Further distribution of this work must maintain attribution to the author(s) and the published article's title, journal citation, and DOI.

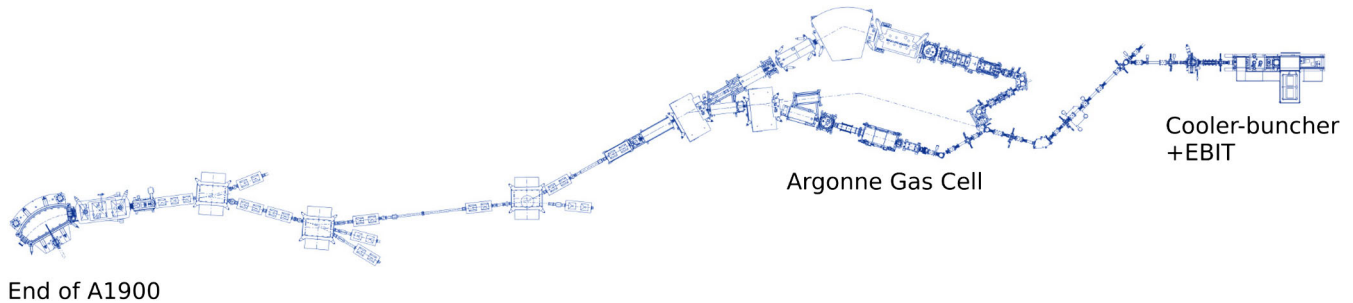


FIG. 1. Schematic layout of the in-flight beam production and beam stopping and charge breeding portions of the National Superconducting Cyclotron Laboratory, from the exit of the A1900 to the exit of the EBIT, with relevant devices labeled. The detectors used in this study were located at these three locations.

^{38}Ca leading to the population of ^{38}K for possible capture [14,15]. While the proton capture on the ground state has been studied [16,17], capture on the isomer may also play a significant nucleosynthesis role, particularly as the decay branch from ^{38}Ca to the ^{38}K isomer is 76.5% [13].

II. BEAM PRODUCTION

Critical to the production of rare isotope beams via fragmentation is a fragment separator or spectrometer; in this work, the A1900 device [18] was used (see Fig. 1). The A1900 has a full momentum acceptance of 5.5%, but in the current measurement the momentum slits were adjusted to allow only 0.5% ($\pm 0.25\%$) acceptance. The transmission and yield of the various reaction products through the A1900 was modeled utilizing the code LISE++ [19], which provides various models for the reaction mechanism and accounts for the various electromagnetic components along the spectrometer beam line, any degrader or stripping foils along the beam path, etc. While LISE++ does not provide estimates of isomeric content, it can be used as a starting point based on estimates for total isotopic production. Based on both LISE++ predictions [19] for total ^{38}K beam production as well as a previous measurement where some ^{38m}K was observed in a ^{38}K beam produced via fragmentation and reacceleration at the National Superconducting Cyclotron Laboratory's ReAccelerated beam (ReA) facility, nominal starting parameters for each device were chosen. The LISE++ version 10.0.6 calculations utilized the universal parameterization of Ref. [20] as the mean fragment velocity model and adopted the settings from the A1900_2016 option and configuration files.

This nominal setting used a ^{40}Ca primary beam from the Coupled Cyclotron Facility (CCF) at 140 MeV/u, impinging onto a beryllium fragmentation target. The A1900 fragment separator [18] was used to select ^{38}K with a momentum acceptance of 0.5%, and the standard suite of A1900 detectors (various beam current monitors, timing scintillators, etc.) was used to determine ^{38}K purity and beam intensity. Reducing the A1900 momentum

acceptance from its maximum 5.5% to 0.5% using the momentum slits allowed for the momentum distribution to be sampled more precisely without each step overlapping. This mixed g + i beam was then stopped in the Argonne Gas Stopper [21] and charge bred to 17+ in the electron-beam ion trap (EBIT) [22,23], which is the optimum charge state for charge breeding efficiency, minimization of contaminants, and matching the q/A range of the ReA linac. Beta decay implantation counters were placed at the end of the A1900, after the Argonne Gas Stopper, and after the EBIT, to measure the ratio of isomer to ground state. Because the lifetimes of the ground state (7.636 min) and isomer (924 ms) are well known [13], beam implantation and subsequent beam-off beta decay curves could be used to determine the ground state to isomer ratio, as shown in Fig. 2. Efficiency-calibrated single-crystal HPGe detectors were also placed near these locations to get a secondary measurement of the ^{38}K ground state beam intensity.

In order to probe the relevant parameter space, several settings were sampled: the momentum distribution of the fragments in the A1900 first segment, the fragmentation

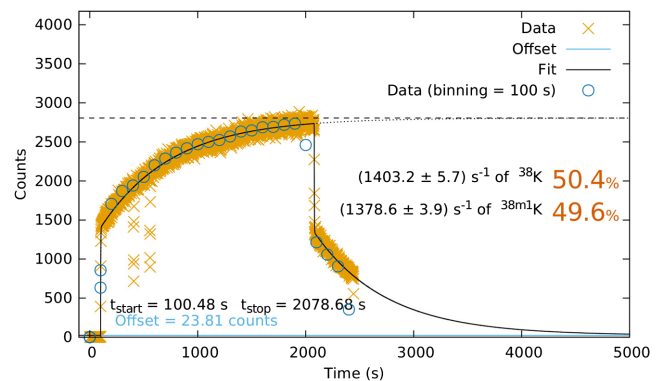


FIG. 2. Example output of the fitting function used to analyze the beta decay curves and determine the isomeric ratio. The ground state and isomer lifetimes are known; the implantation time, beam-off time, run stop time, and offset (background counts due to the remaining decay from the previous decay spectrum measurement) are left as free parameters in the fit.

target thickness, the reaction-separator angle, the gas stopper electric field gradient, and the EBIT charge breeding time.¹

III. ANALYSIS

Results for settings in the A1900 and Argonne Gas Stopper are shown in Fig. 3. A distribution of isomer content as a function of the percent change from the LISE++ [19] predicted optimum $B_{\rho 1,2}$ for the production of ^{38}K with the A1900 is observed,² with the distribution appearing slightly narrower for the thinner fragmentation target (235 mg/cm²) versus the thicker target (987 mg/cm²). The slightly asymmetric shape of this distribution follows closely the shape of the fragment $B\rho$ and momentum curves predicted for $^{40}\text{Ca} + ^9\text{Be} \rightarrow ^{38}\text{K}$ (total production) in LISE++, with an overall offset of +1%. In addition to the samples taken along this momentum distribution, a measurement was taken with the fragmentation target at a higher reaction angle with respect to the beam or separator; to accomplish this, the primary beam tune was adjusted to impinge on the fragmentation target at the largest incident angle allowed by the diameter of the upstream beam pipe (approximately 2°), thus sampling a different angular range with respect to the reaction. Within uncertainties, this change did not affect the isomer production ratio. A peak isomeric ratio of about 56%–57% was observed, at a $B_{\rho 1,2}$ value of about +1% above the LISE++ predicted optimum.

The Argonne Gas Stopper gas cell gradient was also examined. The isomeric fraction produced with the “nominal” gradient setting, which applies a gradient which is nonconstant and discontinuous between anodes, is shown as the dashed line in Fig. 3. Above a certain average gradient (true of both the constant and nominal gradient settings), the time the ions spent slowing in the gas was minimized, hence minimizing the losses to the short-lived isomer.

In addition to the isomer fraction, the absolute beam intensity and transmission efficiency through the stopping and charge breeding steps are also important when planning an experiment using an isomeric beam. After the ions have exited the Argonne Gas Stopper cell, they are injected as a continuous beam into a beam cooler and buncher trap [24] and accumulated for a time equal to the charge breeding time. After accumulation, an ion pulse is injected

¹Because the ratio and not the absolute intensity was the goal of these measurements, each setting was not carefully tuned through each element, so transmission losses did occur. For this reason, we do not report absolute intensities but only basic trends.

² $B_{\rho 1,2}$, or rigidity of the A1900 first segment, prior to the wedge. This setting is based entirely on the fragmentation reaction, and its value is a direct property of how the beam interacts with the target, whereas the rigidity of the second segment may differ from the reaction kinematics based on the use of a wedge or degrader. The entire device was scaled appropriately for each step.

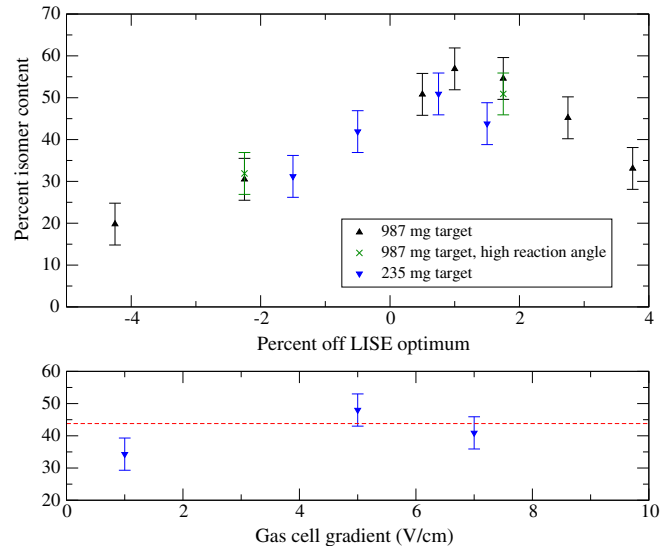


FIG. 3. Isomer content as a percent of the total ^{38}K rate for some of the different parameters varied. Top panel: Isomer content in percent as a function of the percent change, positive or negative, off the LISE++ [19] predicted optimum $B_{\rho 1,2}$ for ^{38}K production with the A1900, for two different fragmentation target thicknesses (thicker target, black; thinner target, blue). The gap around -1% for the thicker (987 mg/cm²) beryllium target is the location of the primary CCF beam. The momentum acceptance of the A1900 for this measurement is $0.5\% (\pm 0.25\%)$, so these data represent the center of the momentum “bite” at each step. In addition, two measurements were taken at a high angle between the fragmentation target and the A1900 for the thicker target, shown as a green \times . The high angle did not alter the results, within uncertainty. Bottom panel: Isomer content in percent as a function of the gradient, in V/cm, in the Argonne Gas Stopper. The red dashed line shows the isomer fraction when using the “nominal” gas cell gradient settings, which is a nonconstant and noncontinuous field. The three points, all taken with the thinner fragmentation target, represent constant gradient settings.

into the EBIT for charge breeding. Figure 4 shows the isomer fraction (beginning from the optimum setting from the A1900), ^{38}K purity, and intensity of contaminants with the same A/q for the different EBIT charge breeding times sampled. A loss of approximately 33% total beam intensity was seen between charge breeding times of 150 and 1500 ms, but with a corresponding drop in the isomeric fraction of more than a factor of 2. Breeding to optimize a different extracted charge (other than 17+) would alter this ratio, as it changes the breeding times. However, due to the various constraints mentioned previously, not all charge states would be feasible for beam production. The intensity of the contaminants is a function of the breeding time and not of the incoming (stopping) beam rate, so increased rates of the beam of interest would also result in higher purity. This measurement observed attenuated beam rates of up to ~ 8000 pps, but the attenuators, nominally factors of 10, 100, etc., are not precisely calibrated, and therefore an absolute intensity cannot be obtained. However, some

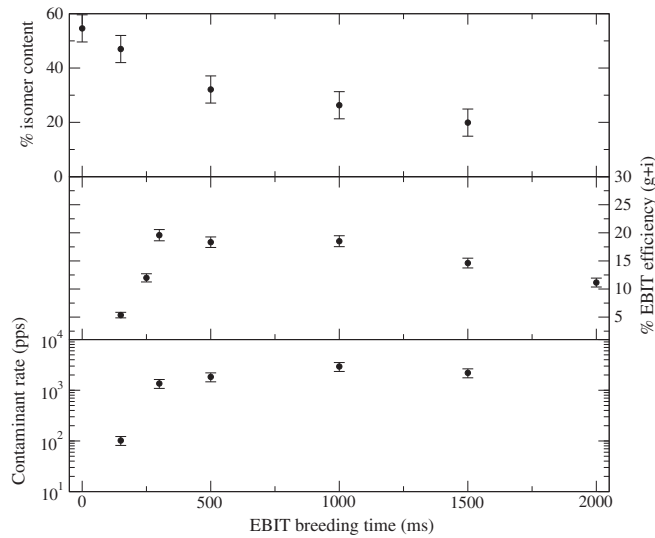


FIG. 4. Top panel: Isomer content as a percent of the total ^{38}K rate for different breeding times of the EBIT. The changing ratio follows the general trend dictated by the two different lifetimes, but additional losses such as ions escaping the EBIT trapping potentials during the charge breeding process can be observed. A breeding time of “zero” represents the starting isomer percentage prior to breeding; this ignores the additional decay time spent during accumulation in the cooler buncher. Middle panel: Percent efficiency for extracting the total ^{38}K beam (ground state plus isomer) from the EBIT. Bottom panel: Rate of contaminants, mostly stable ^{38}Ar from the EBIT residual gas, extracted from the EBIT for the different breeding times.

conclusions can be drawn. The maximum unattenuated rate of contaminants arising from charge breeding is on the order of 3000 pps (cf. Fig. 4), an effect of the breeding time and not the rate of the stopped beam [23]. This indicates that the rate of contaminants in the beam of interest should be smaller than $\sim 3000/8000$ by at least the true attenuation factor, in addition to any gains in the intensity of the incoming (stopping) beam. Because of the need to charge breed in order to reaccelerate, the maximum isomeric content in an in-beam measurement would be less than the peak seen at the exit of the A1900.

IV. CONCLUSION

Beams of ground state and isomeric content $^{38}\text{K}/^{38m}\text{K}$ were successfully produced via fast fragmentation and separation using the A1900 separator at the National Superconducting Cyclotron Laboratory. Changing the charge breeding time in the EBIT proved the most effective method of varying the percentage of the beam which was in the isomeric state without substantial losses in intensity. Combining an A1900 setting with a smaller isomeric fraction production with a longer EBIT breeding time (~ 2 s) could provide an isomeric content as low as 5%, enabling a roughly factor of 10 difference in isomeric fraction for similar beam intensities. The isomer content

was maximized a small percentage off the LISE++ predicted optimum rigidity $B_{\rho 1,2}$ regardless of the fragmentation target thickness. The technique of producing isomeric beams with fast fragmentation and separation appears promising, though studies of other low-spin, low-excitation energy systems should be undertaken to better understand the underlying mechanism of the isomer population in fragmentation reactions.

ACKNOWLEDGMENTS

K. A. C. thanks D. Stracener for helpful discussions in preparing the manuscript. Research was sponsored by the Laboratory Directed Research and Development Program of Oak Ridge National Laboratory, managed by UT-Battelle, LLC, for the U.S. Department of Energy. This work was supported by the U.S. Department of Energy, Office of Science, Office of Nuclear Physics under Contract No. DE-AC05-00OR22725, and the National Science Foundation under Grant No. PHY-1430152 (JINA Center for the Evolution of the Elements) and Grant No. PHY-1565546 (National Superconducting Cyclotron Laboratory).

- [1] A. Gorelov *et al.*, Scalar Interaction Limits from the $\beta - \nu$ Correlation of Trapped Radioactive Atoms, *Phys. Rev. Lett.* **94**, 142501 (2005).
- [2] J. Van Roosbroeck *et al.*, Unambiguous Identification of Three β -Decaying Isomers in ^{70}Cu , *Phys. Rev. Lett.* **92**, 112501 (2004).
- [3] I. Stefanescu *et al.*, Coulomb Excitation of $^{68,70}\text{Cu}$: First Use of Postaccelerated Isomeric Beams, *Phys. Rev. Lett.* **98**, 122701 (2007).
- [4] D. Santiago-Gonzalez (private communication).
- [5] S. Almaraz-Calderon *et al.*, Study of the $^{26}\text{Al}^m(d, p)^{27}\text{Al}$ Reaction and the Influence of the $^{26}\text{Al}0^+$ Isomer on the Destruction of ^{26}Al in the Galaxy, *Phys. Rev. Lett.* **119**, 072701 (2017).
- [6] G. Doukellis and J. Rapaport, The $^{26}\text{Mg}(p, n)^{26}\text{Al}$ and $^{23}\text{Na}(\alpha, n)^{26}\text{Al}$ reactions near threshold, *Nucl. Phys.* **A467**, 511 (1987).
- [7] S. Pal and R. Palit, Angular momentum population in fragmentation reactions, *Phys. Lett. B* **665**, 164 (2008).
- [8] S. Go *et al.*, Annual Report No. CNS-REP-90, 2011, p. 32.
- [9] R. Yokoyama *et al.*, Annual Report No. CNS-REP-90, 2011, p. 34.
- [10] A. D. Bacelar *et al.*, The population of metastable states as a probe of relativistic-energy fragmentation reactions, *Phys. Lett. B* **723**, 302 (2013).
- [11] M. Bowry *et al.*, Population of high-spin isomeric states following fragmentation of ^{238}U , *Phys. Rev. C* **88**, 024611 (2013).
- [12] M. Block *et al.*, Discovery of a nuclear isomer in ^{65}Fe with PenningTrap mass spectrometry, *Phys. Rev. Lett.* **100**, 132501 (2008).

- [13] J. A. Cameron and B. Singh, Nuclear Data Sheets for $A = 38$, *Nucl. Data Sheets* **109**, 1 (2008).
- [14] J. L. Fisker, E. F. Brown, M. Liebendörfer, F.-K. Thielemann, and M. Wiescher, The reactions and ashes of thermonuclear explosions on neutron stars, *Nucl. Phys.* **A752**, 604 (2005).
- [15] J. L. Fisker, H. Schatz, and F.-K. Thielemann, Explosive hydrogen burning during Type I x-ray bursts, *Astrophys. J. Suppl. Ser.* **174**, 261 (2008).
- [16] G. Lotay *et al.*, Direct Measurement of the Astrophysical $^{38}\text{K}(p,\gamma)^{39}\text{Ca}$ Reaction and Its Influence on the Production of Nuclides toward the End Point of Nova Nucleosynthesis, *Phys. Rev. Lett.* **116**, 132701 (2016).
- [17] G. Christian *et al.*, Direct measurement of astrophysically important resonances in $^{38}\text{K}(p,\gamma)^{39}\text{Ca}$, *Phys. Rev. C* **97**, 025802 (2018).
- [18] D. Morrissey, B. Sherrill, M. Steiner, A. Stolz, and I. Wiedenhoefer, Commissioning the A1900 projectile fragment separator, *Nucl. Instrum. Methods Phys. Res., Sect. B* **204**, 90 (2003).
- [19] O. B. Tarasov and D. Bazin, LISE++: Exotic beam production with fragment separators and their design, *Nucl. Instrum. Methods Phys. Res., Sect. B* **376**, 185 (2016).
- [20] O. Tarasov, Analysis of momentum distributions of projectile fragmentation products, *Nucl. Phys.* **A734**, 536 (2004).
- [21] K. Cooper, C. S. Sumithrarachchi, D. J. Morrissey, A. Levand, J. A. Rodriguez, G. Savard, S. Schwarz, and B. Zabransky, Extraction of thermalized projectile fragments from a large volume gas cell, *Nucl. Instrum. Methods Phys. Res., Sect. A* **763**, 543 (2014).
- [22] M. A. Levine, R. E. Marrs, J. R. Henderson, D. A. Knapp, and M. B. Schneider, The electron beam ion trap: A new instrument for atomic physics measurements, *Phys. Scr.* **T22**, 157 (1988).
- [23] A. Lapiere *et al.*, First two operational years of the electron-beam ion trap charge breeder at the National Superconducting Cyclotron Laboratory, *Phys. Rev. Accel. Beams* **21**, 053401 (2018).
- [24] S. Schwarz, G. Bollen, R. Ringle, J. Savory, and P. Schury, The LEBIT ion cooler and buncher, *Nucl. Instrum. Methods Phys. Res., Sect. A* **816**, 131 (2016).